

**Supplementary information**  
**for**  
  
**Folate-decorated Amphiphilic Cyclodextrins as**  
  
**Cell-Targeted Nano-phototherapeutics**

*Roberto Zagami,<sup>†,⊥</sup> Valentina Rapozzi,<sup>‡,⊥</sup> Anna Piperno,<sup>§,⊥</sup> Angela Scala,<sup>§</sup> Claudia Triolo,<sup>||</sup>  
Mariachiara Trapani,<sup>†</sup> Luigi E. Xodo,<sup>‡</sup> Luigi Monsù Scolaro,<sup>§</sup> and Antonino Mazzaglia<sup>\*†</sup>*

*<sup>†</sup>CNR-ISMN, Istituto per lo Studio dei Materiali Nanostrutturati c/o Dipartimento di Scienze  
Chimiche, Biologiche, Farmaceutiche ed Ambientali, Università di Messina, Viale F. Stagno  
d'Alcontres 31, Messina 98166, Italy*

*<sup>‡</sup>Dipartimento di Area Medica, Università di Udine, P.le Kolbe 4, Udine 33100, Italy*

*<sup>§</sup>Dipartimento di Scienze Chimiche, Biologiche, Farmaceutiche ed Ambientali, Università di  
Messina, Viale F. Stagno d'Alcontres 31, Messina 98166, Italy*

*<sup>||</sup>Dipartimento di Scienze Matematiche e Informatiche, Scienze Fisiche e Scienze della Terra.  
Università di Messina, Viale F. Stagno d'Alcontres, 31, 98166 Messina*

## **Table of Contents**

<b>Synthesis and characterization of Ada-FA</b>	4
<b>Scheme S1.</b> Synthetic strategy for the preparation of Ada-FA	6
<b>Trasmission Electron Microscopy</b>	7
<b>Time resolved fluorescence</b>	7
<b>Release studies</b>	9
<b>Western Blot Analysis.</b>	9
<b>Intracellular ROS detection</b>	10
<b>Double-Fluorescent nanoassemblies preparation</b>	11
<b>Confocal microscopy studies on double fluorescent nanoassemblies</b>	11
<b>Figure S1.</b> Size distribution and $\zeta$ -potential of SP and SAP in ultrapure water	12
<b>Table S1.</b> Properties of S and SA	13
<b>Figure S2.</b> Trasmission Electron Microscopy images	13
<b>Figure S3.</b> Time resolved fluorescence decay of Ada-FA and of SA	14
<b>Table S2.</b> Fluorescence emission lifetimes of Ada-FA and SA	14
<b>Figure S4.</b> Absorbance calibration curves of Pheo, Ada-FA and SP and SAP	15

<b>Figure S5.</b> Release kinetics of Pheo from SAP	15
<b>Figure S6.</b> Calibration curve by fluorescence emission for Pheo in PBS	16
<b>Figure S7.</b> Stability studies in biological relevant media by UV/vis spectroscopy	16
<b>Figure S8.</b> Stability of SP and SAP in aqueous dispersion by $\zeta$ -potential measurements	17
<b>Figure S9.</b> RNO bleaching kinetics of Pheo, SP and SAP	17
<b>Figure S10.</b> Different expression of folate receptor protein (FR- $\alpha$ ) by western blotting	18
<b>Figure S11.</b> Confocal microscope images of cells treated with Pheo, SP and SAP	18
<b>Figure S12.</b> Fluorescence emission spectra of Dns-SP in aqueous solution	19
<b>Figure S13.</b> Confocal microscope images of cells treated with Pheo, Dns-SP and Dns-SAP	20
<b>Figure S14.</b> Metabolic activity (%) of cells treated with Pheo, SP and SAP	21
<b>Figure S15.</b> Metabolic activity (%) of cells treated with S, Ada-FA and SA	22
<b>Figure S16.</b> Intracellular ROS of cells treated with Pheo, SP and SAP	22
<b>References</b>	23

## Synthesis and characterization of Ada-FA.

**Materials.** N,N'-carbonyldiimidazole (CDI), N-(3-dimethylaminopropyl)-N'-ethylcarbodiimide hydrochloride (EDC), N,N-diisopropylethylamine (DIPEA), Hydroxybenzotriazole (HOBt) and all the reagents and solvents (analytical grade) were purchased from Sigma-Aldrich (Milano, Italy).

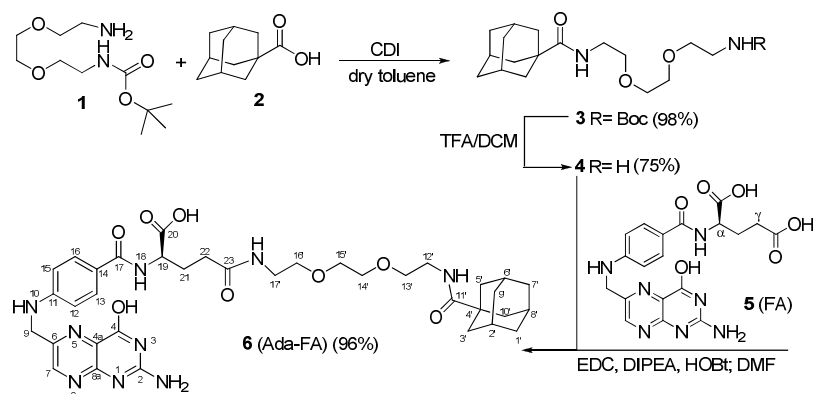
**Synthesis of N-(2-(2-(2-aminoethoxy)ethoxy)ethyl)adamantane-1-carboxamide (4).** Adamantyl carboxylic acid (**2**, Scheme S1) (180 mg, 1 mmol) was added to a round-bottom flask containing dry toluene (20 mL) and fitted with a reflux condenser, a dry Argon inlet, and a magnetic stirrer. The solution was heated up to 60 °C and stirred. CDI (169 mg, 1 mmol) was added to the solution and stirred until the CO<sub>2</sub> evolution had ceased. The solution was heated for a further 30 min and purged with argon. Tert-butyl 2-(2-(2-aminoethoxy)ethoxy)ethylcarbamate<sup>1</sup> (**1**, Scheme S1) (250 mg 1.0 mmol) was added to the solution and allowed to stir at 60 °C for a further 2 h and then cooled to room temperature. The reaction mixture was concentrated in vacuo, and the remaining clear liquid was dissolved in dichloromethane (DCM) and washed three times with water (3 x 10 mL). The washed DCM solution was dried with anhydrous Na<sub>2</sub>SO<sub>4</sub>, filtered, and concentrated to give 408 mg of (**3**, Scheme S1) as a clear oil. *Ada-LinkerNHBoc* (**3**) (C<sub>22</sub>H<sub>38</sub>N<sub>2</sub>O<sub>5</sub>) was obtained in nearly quantitative yield (98%) and was used without further purification. <sup>1</sup>H NMR (500 MHz, CDCl<sub>3</sub>): δ = 1.36 (s, 9H), 1.61-66 (m, 6H, 1,7,9-H), 1.76 (m, 6H, 3,5,10-H ), 1.96 (s, 3H, 2,6,8-H), 3.25 (m, 2H, 17-H), 3.35 (m, 2H, 12-H), 3.50 (m, 4H, 14,15-H ), 3.55 (m, 4H, 13,16-H), 4.95 (s, 1H, NH), 6.15 (s, 1H, NH). To a solution of (**3**) (380 mg, 1 mmol) in DCM (2 mL), 3 mL of trifluoroacetic acid (TFA) was added dropwise and the reaction mixture was stirred at room temperature for 2 h. The reaction mixture was washed with a solution of KOH (10 %) and the organic phases were dried, filtered, and concentrated. The

crude product was purified by column chromatography using DCM/ethanol in 2:1 mixture; (silica gel, 1%  $\text{NH}_3$ ,  $R_f = 0.25$ ). *N*-(2-(2-(2-aminoethoxy)ethoxy)ethyl)adamantane-1-carboxamide (**4**, Scheme S1) was obtained as sticky white solid (235 mg, 0.75 mmol, 75 % yield). Adopting our two-step procedure, (**4**) was obtained in good yield and in mild conditions, whereas the literature one-step procedures<sup>2, 3</sup> require the use of hazardous adamantanecarbonyl chloride in controlled conditions (*i.e.* -78 °C). NMR spectra matched those reported in the literature.<sup>4,5</sup> MALDI-TOF ( $m/z$ ): 311.23 [ $\text{MH}^+$ ] and [ $\text{MNa}^+$ ] 333.23 cld for  $\text{C}_{17}\text{H}_{30}\text{N}_2\text{O}_3$  310.23.

**Synthesis of Ada-FA (6).** FA (**5**, Scheme S1) (194 mg, 0.41 mmol) was solubilised in anhydrous DMF (10 mL) under sonication (5 min). To the stirring solution of (**5**), EDC (78 mg, 0.41 mmol) and DIPEA (0.0725 mL, 0.82 mmol) were added and the reaction mixture was stirred in the dark for 1 h. Then, HOBt (55.4 mg, 0.41 mmol) was added and the reaction mixture was further stirred in the dark for 1 h. A 1 mL solution of (**4**) (126 mg, 0.41 mmol) in anhydrous DMF was added and the reaction mixture was stirred in the dark for 24 h at room temperature. The formed yellow precipitate was recovered by filtration under vacuum and it was washed several times with organic solvents (DMF, chloroform, acetone and diethylether). The solid material was dried to give Ada-FA (**6**, Scheme S1) as a yellow powder (290 mg, 96 % yield) as inseparable mixture of  $\gamma$ - and  $\alpha$ -regioisomer.  $^1\text{H}$  and COSY NMR experiments indicated an almost exclusive  $\gamma$ -conjugation of FA whereas the amount of the  $\alpha$ -regioisomer was negligible (1-1.5 %).  $^1\text{H}$  NMR (500 MHz,  $\text{DMSO-d}_6$ )  $\delta$  = 1.61-1.66 (m, 6H, H-1', H-7', H-9'), 1.77 (d, 6H,  $J = 2.8$  Hz, H-3', H-5', H-10'), 1.98 (s, 3H, H-2', H-6', H-8'), 2.05 (m, 2H, H-21), 2.23 (m, 2H, H-22), 3.13-3.20 (m, 4H, H-12', H-17'), 3.25-3.40 (m, 8H, H-13', H-14', H-15', H-16), 4.32 (m, 1H, H-19), 4.46 (d, 2H,  $J = 3.0$  Hz, H-9), 6.61 (d, 2H,  $J = 5.9$  Hz, H-12, H-15), 6.90 (t, 1H, NH-10,  $J = 3.0$  Hz), 7.30 (bs, 1H, NHCO-11'), 7.55 (s, 1H, OH), 7.60 (d, 2H,  $J = 5.9$  Hz, H-13, H-

16), 7.95 (bs, 1H, NHCO-23), 8.05 (d, 1H, NH-18,  $J = 2.0$ ), 8.61 (s, 1H, H-7), 11.43 (bs, 1H, OH).  $^{13}\text{C}$  NMR (125 MHz, DMSO- $d_6$ )  $\delta = 25.9$ , 26.4 (CH<sub>2</sub>-Ada), 26.5 (C21), 28.1 (C6', C8', C2'), 30.8 (C22), 36.6 (C1', C7', C9'), 36.7 (C4'-Ada), 38.9 (C12', C17'), 39.1 (CH<sub>2</sub>-Ada), 46.3 (C9), 52.4 (C19), 69.4 (C13', C16'), 69.9 (C14', C15'), 111.9 (C12, C15), 121.7 (C11), 128.3 (C4a), 129.5 (C13, C16), 149.0 (C7), 151.3 (C8a), 151.5 (C6), 154.2 (C14), 159.0 (C2), 162.9 (C4), 166.9 (C17), 174.2 (C20), 174.4 (C23), 177.7 (C11'). MALDI-TOF ( $m/z$  734.02 [ $\text{MH}^+$ ] and [ $\text{MNa}^+$ ] 755.95 calcd for  $\text{C}_{36}\text{H}_{47}\text{N}_9\text{O}_8$  733.35).

Differently to literature procedures,<sup>4, 5</sup> the conjugation of FA to the linker (**4**) was performed in the last synthetic step, overcoming the drawback of the poor solubility of FA conjugates in all organic solvents (except DMSO), and allowing purification of Ada-FA (**6**) by repetitive washing with organic solvents. MALDI-TOF analysis unambiguously confirmed the expected mass values for **6**, exhibiting the values of protonated and sodiated species at 734.02  $m/z$  ( $\text{MH}^+$ ) and 755.95  $m/z$  ( $\text{MNa}^+$ ), respectively. The almost exclusive  $\gamma$ -conjugation was assessed by mono- and bi-dimensional NMR experiments ( $^1\text{H}$  and  $^{13}\text{C}$  spectra; COSY, HSQC and HMBC). The characteristic FA signals at 2.05, 2.23, 4.32, 4.46, 6.61, 6.95, 7.60, 8.05, 8.61, 11.43, due to H-21, H-22, H-19, H-9, H-12/16, H-2, H-13/15, H-18, H-7, H-20 respectively, have been detected. The signals of adamantane moiety appeared at 1.61-1.66, 1.77 and 1.98 ppm. The coupling of FA with free amine group of (**4**) gave the expected downfield shift of the signal at 2.88 ppm (triplet of H-17') to 3.13-3.20 ppm. In the HMBC spectrum, the correlation between the signal at 174.2 ppm and the signal at 4.2 ppm (H-19) and the absence of any further correlation unambiguously indicated that the signal at 174.2 ppm can be attributed to the free  $\alpha$ -carboxylic group. Moreover, the signal at 174.4 ppm can be attributed to the C-23 amide group due to the correlation with the signal at 2.27 ppm (H-22).



**Scheme S1.** Synthetic strategy for the preparation of Ada-FA.

**Transmission Electron Microscopy.** Nanoassemblies morphology was investigated using a transmission electron microscopy (TEM), JEM2100 LaB6, operating at 200 kV at University of Exeter (UK). TEM samples were prepared to place ten drops of the sample dispersed in H<sub>2</sub>O (~0.5 mg/mL) by sonication (20 min in an ultrasound bath), on 300 mesh holey-carbon coated copper grids.

**Time resolved fluorescence.** Time resolved fluorescence emission measurements were performed on a Jobin Yvon-Spex Fluoromax 4 spectrofluorimeter using Time-Correlated Single-Photon Counting technique. A NanoLED ( $\lambda = 390$  nm) has been used as excitation source. Time-resolved fluorescence anisotropy,  $r(t)$ , is defined using the following expression:

$$r(t) = \frac{I_{vv}(t) - I_{vh}(t)}{I_{vv}(t) + 2I_{vh}(t)} = \frac{I_d(t)}{I_s(t)} \quad (1)$$

where “ $d$ ” and “ $s$ ” refer to “sum” and “difference”. The anisotropy measurements were collected as the emission polarized was switched between parallel and perpendicular positions relative to the vertically oriented excitation polarized till a minimum peak difference of 10000 counts was

reached. A correction measurement ( $g$ -factor) was experimentally determined, involving the use of horizontally polarized excitation incident on the sample, to adjust for the polarization bias of the detection instrumentation. The resulting sum and difference decays were analyzed using the impulse reconvolution method provided by the instrument's DAS6 software analysis package where in the simplest case the change of anisotropy with time is given from the following exponential decay fit:

$$r(t) = r_0 \exp(-t/\tau_r) \quad (2)$$

where  $r_0$  is the initial anisotropy and ranges from 0.4 (parallel transition dipoles) to -0.2 (perpendicular dipoles).  $\tau_r$  is the rotational correlation time, which can be considered a measure of the order-disorder process. If the fluorophore is not fully free to rotate, then a non-zero limiting anisotropy ( $r_\infty$ ) can be considered. The time-resolved measurement is then described as follows,

$$r(t) = r_\infty + (r_0 - r_\infty) \exp(-t/\tau_r) \quad (3)$$

$$\tau_r = \frac{V\eta}{kT} \quad (4)$$

where  $r$  is the anisotropy,  $r_\infty$  is the anisotropy at infinite time,  $r_0$  is the initial anisotropy.  $\tau_r$  is the rotational correlation time, which can be determined and related to the effective volume of a molecule ( $V$ ) and the local viscosity ( $\eta$ ). Also  $T$  is absolute temperature and  $k$  is Boltzman's constant.



**Release Studies.** SAP nanoassemblies dispersed in PBS (2 mL) were put into a dialysis tube (Spectra/Por dialysis bags, MWCO 3.5-5 kDa) and immersed into 10 mL of PBS 10 mM, (pH = 7.4) at  $37 \pm 0.1$  °C under continuous stirring (100 rpm), in presence of a 10 % v/v of Tween® 80 as Pheo solubilizer. At fixed times, 2 mL of release medium was withdrawn and replaced with an equal volume of fresh PBS-Tween® 80 and analyzed by fluorescence spectroscopy. The calibration curve of Pheo was obtained in PBS enriched with 10% v/v of Tween® 80 by plotting the values of fluorescence intensity at 675 nm vs Pheo concentration in the range 0.5-3.0  $\mu$ M. The amount of Pheo released was expressed as percentage ratio between the weight of released Pheo and the total amount of Pheo entrapped. At the end of the release processes, all the collected volumes were lyophilized and the residues were solubilized in DCM (2 mL) and analyzed by UV/Vis spectroscopy. The stability behavior of free Pheo was also studied by a control experiment in the same conditions. Pheo was dissolved in DMSO/PBS (1:20) and the dialysis bag was put in contact with the external release medium (PBS enriched with Tween® 80).

**Western Blot Analysis.** The protein extracts (40  $\mu$ g), obtained from whole cell lysates, were subjected to electrophoresis on 12 % SDS-PAGE and transferred to a nitrocellulose membrane at 70 V for 2 h. The filter was blocked for 1 h with PBS-0.01 % Tween (Sigma-Aldrich, Milan, Italy) containing 5 % dry non-fat-milk, and then incubated at 4 °C overnight with the primary antibody [rabbit polyclonal anti-FOLR1 (Thermo Scientific, PA5-24186; Rockford, USA) diluted 1 : 1000. The expression of  $\beta$ -actin, used as an internal control, was detected with a mouse monoclonal anti  $\beta$ -actin (Ab-1, CP01, Calbiochem, Merck Millipore, Darmstadt, Germany), diluted 1 : 10000. The filters were incubated for 1 h with the secondary antibodies [anti-rabbit IgG, diluted 1 : 4000 (Calbiochem, Merck Millipore, Darmstadt, Germany), anti-

mouse IgM, diluted 1:5000 (Calbiochem, Merck Millipore, Darmstadt, Germany). Each secondary antibody was coupled to horseradish peroxidase (HPR). For the detection of the proteins, we used ECL (enhanced chemiluminescence) reagents (Super SignalRWest PICO, and Super SignalRWest FEMTO, ThermoFisher Scientific Pierce, Rockford, USA). The exposure length depended on the antibodies used and was usually between 30 s and 5 min. The protein levels were quantified by the Image Quant TL Version 2003 software (Amersham).

### **Intracellular ROS detection**

PC3 and MCF-7 were plated at density of  $2 \times 10^5$  and  $1.8 \times 10^5$  cells/well, respectively, in a 12-well plate. The day after, the cells were treated with SAP, SP or Pheo at various concentrations. After an overnight incubation in the dark, the cells were irradiated with red led at a fluence of  $0.9 \text{ J/cm}^2$ . After 1 h, ROS were measured by incubating the cells in white medium DMEM (Biowhittaker LONZA, Milan, Italy) without serum for 30 minutes at 37°C with 5 mM of 5-(and 6)-chloromethyl-2',7'-dichlorodihydrofluorescein diacetate, acetyl ester CM-H<sub>2</sub>DCFDA (C6827, Molecular Probes, Invitrogen, Milan, Italy). CM-H<sub>2</sub>DCFDA was metabolized by nonspecific esterases to the nonfluorescence product of 5-(and 6)-chloromethyl-2',7'-dichlorodihydrofluorescein diacetate, acetyl ester, which was oxidized to the fluorescent product, DCF, by ROS. The cells were washed twice in PBS, trypsinized, suspended in PBS and measured for the ROS content by FACS (FACScalibur, Becton Dickinson, San Jose, CA). The signal was detected by FL1 channel in log scale (x-axis of plot). The samples were analyzed with the FlowJo program.

**Double-Fluorescent nanoassemblies preparation.** To detect both photosensitiser drug and carrier in the cells, we used a fluorescent cyclodextrin aggregate of a dansylated amphiphilic cyclodextrin (SC6Dns) formulated in the presence of an equimolar amount of cationic amphiphilic CD (SC6NH<sub>2</sub>), according to our previous reported procedure.<sup>6</sup> In order to obtain double fluorescent nanoassemblies, with the same molar ratio of SP and SAP systems, all the component of the system (S, SC6NH<sub>2</sub>, SC6Dns, Ada-FA and Pheo) were mixed in DCM in a single step. By evaporation of this solution an organic film was obtained. This was hydrated with PBS (10 mM, pH = 7.4) at r.t. and sonicated in ultrasonic bath for about 20 minutes. The total amount of aCD contained into nanoassemblies was 200  $\mu$ M ([SC6NH<sub>2</sub>] = [SC6Dns] = 10  $\mu$ M, [S] = 180  $\mu$ M). The formation of mixed double fluorescent nanoassemblies SC6NH<sub>2</sub>@SC6Dns/SP (Dns-SP) and SC6NH<sub>2</sub>@SC6Dns/SAP (Dns-SAP) was monitored through fluorescence spectroscopy (see Fig. S12).

**Confocal microscopy studies on double fluorescent nanoassemblies .** MCF-7 and PC3 cells were seeded on 19 mm coverslips in a 6-well plate at a density of  $3 \times 10^5$  and  $4 \times 10^5$  cells respectively. The cells were treated with Dns-SAP and Dns-SP ([Pheo]= 2.5  $\mu$ M) and incubated in the dark for 3 h in a medium without serum. After this time the glasses were prepared. The cells were washed twice with PBS, fixed with 3% paraformaldehyde (PFA) in PBS for 20 min. After washing with 0.1 M glycine, containing 0.02% sodium azide in PBS to remove PFA, and Triton X-100 (0.1% in PBS), the glasses were analyzed using a Leica TCS SP confocal laser scanning system on inverted microscope DMIRBE (Leica Microsystems, Heidelberg, Germany). The uptake of the double-fluorescent nanoassemblies was measured monitoring the red fluorescence of Pheo, exciting with 543 line of He-Ne laser and detecting with 585/630 emission

filters, and green fluorescence of Dns-amphiphilic CD, exciting with 488 nm line Argon-Ion laser and detecting with emission bandpass filters 500/530 nm.

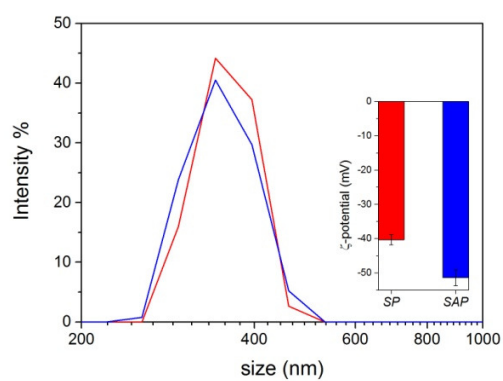


**Figure S1.** Size distribution and  $\zeta$ -potential of SP (red) and SAP (blue) nanoassemblies in ultrapure water.

**Table S1.** Overall Properties of SA in comparison with unloaded S (see Experimental methods): Mean Hydrodynamic Diameter ( $D_H$ ) and Polydispersity Index (PDI) in ultrapure water, PBS (10 mM, pH 7.4) and in aqueous solution of NaCl (0.9 wt %), respectively, and  $\zeta$ -Potential in ultrapure water. SD was calculated on three different batches.

System	Dispersion medium	$D_H$ (nm $\pm$ SD) (%) <sup>a,b</sup>	PDI	$\zeta$ (mV $\pm$ SD)	Theoretical drug loading (%)	Actual loading (%) <sup>c</sup>	EE (%) <sup>d</sup>
S	H <sub>2</sub> O	121 $\pm$ 10(59) <sup>a</sup>	$\leq 0.16$	-36 $\pm$ 7.2			
		8 $\pm$ 0.8 (41) <sup>a,b</sup>	$\leq 0.20$				
SA	H <sub>2</sub> O	303 $\pm$ 75(90) <sup>a</sup>	-	-48 $\pm$ 5.4	8.08	8.0 $\pm$ 0.05	99 $\pm$ 0.6
		64 $\pm$ 12(10) <sup>a,b</sup>	$\leq 0.38$				

<sup>a</sup>Size with corresponding intensity % distribution; <sup>b</sup>Size with corresponding number % distribution: in the presence of two families of nanoassemblies, number % for smaller nanoassemblies is  $\cong 99.9\%$ . <sup>c</sup>Actual loading is expressed as the amount of Ada-FA (mg) encapsulated per 100 mg of nanoassembly. <sup>d</sup>Entrapment Efficiency percentage (EE %): ratio between actual and theoretical loading x 100.

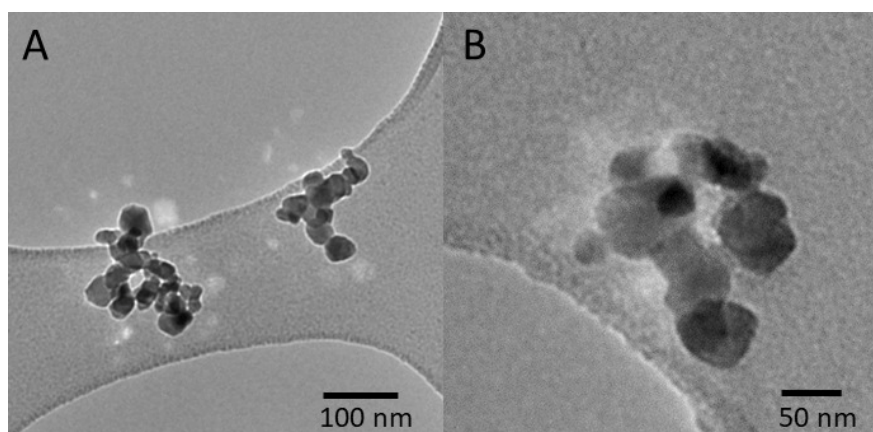


**Figure S2.** Representative TEM images of SAP at low (a) and higher magnification (b)

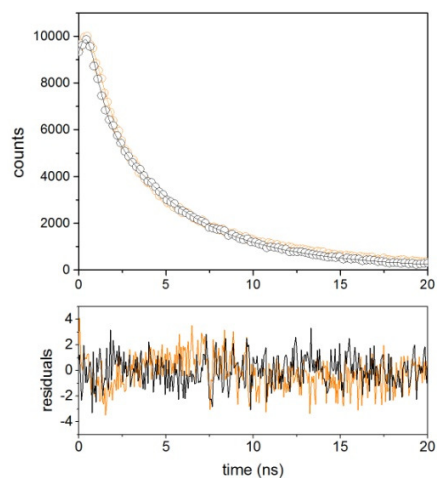


**Figure S3.** Time resolved fluorescence decay of Ada-FA (orange line) in MeOH and of SA (black line) in aqueous solution at r.t ( $\lambda_{\text{em}} = 455 \text{ nm}$ ,  $\lambda_{\text{exc}} = 390 \text{ nm}$ ).

**Table S2.** Fluorescence emission lifetimes of Ada-FA and SA nanoassemblies.

System <sup>a</sup>	$\tau_1$ (ns)	$\tau_2$ (ns)	$\tau_1 A_1$ (%)	$\tau_1 A_2$ (%)
Ada-FA <sup>b</sup>	$1.4 \pm 0.01$	$7.5 \pm 0.02$	36	64
SA <sup>c</sup>	$3.9 \pm 0.08$	$8.8 \pm 0.06$	60	40

<sup>a</sup>Fluorescence lifetimes were measured at  $\lambda_{\text{em}} = 455 \text{ nm}$  ( $\lambda_{\text{exc}} = 390 \text{ nm}$ ).  $A_i$  is the amplitude of the intensity decay <sup>b</sup>MeOH; <sup>c</sup> aqueous solution.

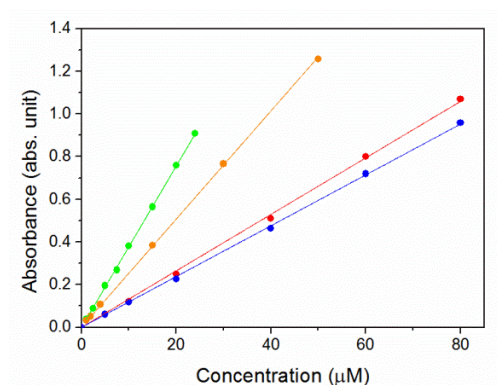


**Figure S4.** Absorbance calibration curves for free Pheo in DCM (green circles), SP (red circles) and SAP (blue circles) dispersed in aqueous solution, and for Ada-FA (orange circles) in MeOH.  $\epsilon_{667\text{nm-Pheo(DCM)}} = 37790 \pm 191 \text{ M}^{-1}, \text{ cm}^{-1}$ ;  $\epsilon_{282\text{nm-Ada-FA(MeOH)}} = 25370 \pm 385 \text{ M}^{-1}, \text{ cm}^{-1}$ ;  $\epsilon_{670\text{nm-SP(PBS)}} = 13240 \pm 112 \text{ M}^{-1}, \text{ cm}^{-1}$ ;  $\epsilon_{670\text{nm-SAP(PBS)}} = 11910 \pm 72 \text{ M}^{-1}, \text{ cm}^{-1}$ .

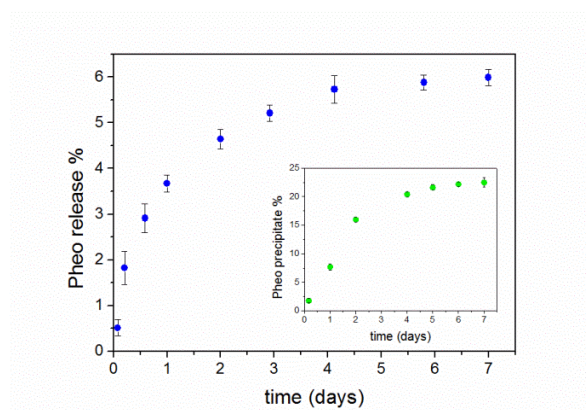


**Figure S5.** Release kinetics of Pheo from SAP (blue circle) dispersed in PBS (10 mM) at pH 7.4 and 37 °C. In inset the stability profile of Pheo (dispersed in PBS at pH 7.4 and 37 °C) vs time. The external medium used for dialysis was PBS (10 mM) at pH 7.4 enriched with 10 % v/v of Tween® 80. Free Pheo and Pheo in NA dispersions was 70 μM. Data are reported as mean of three independent experiments  $\pm$  SD.

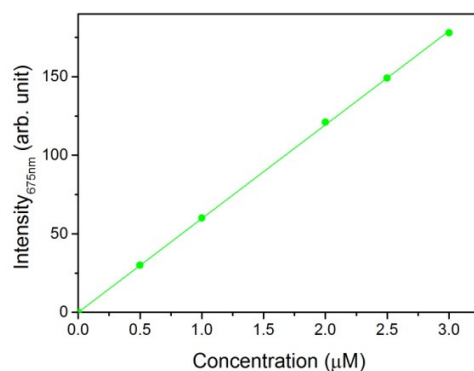


**Figure S6.** Calibration curve by fluorescence emission for Pheo in PBS (10 mM, pH 7.4) in the presence of a 10 % v/v of Tween® 80 ( $\lambda_{ex}$ . 440 nm, r.t.).

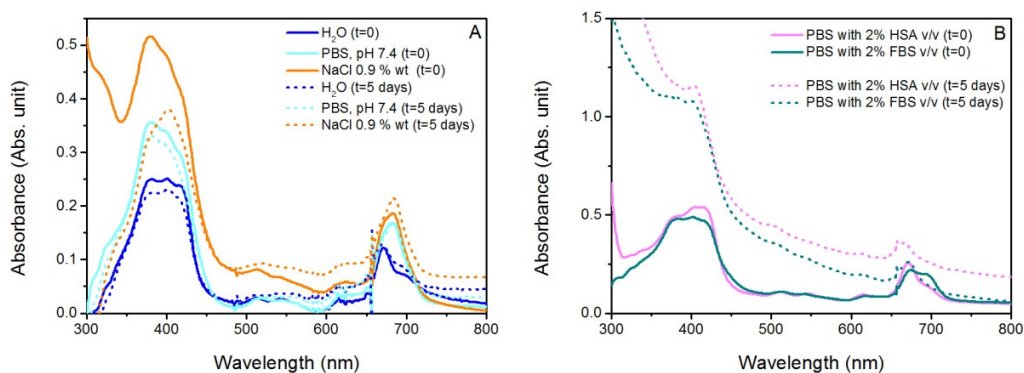


**Figure S7.** UV/vis spectra of SAP at  $t = 0$  (solid lines) and  $t = 1$  week (dotted lines) in (A) aqueous solution (blue lines), PBS solution pH 7.4 (cyan lines) and NaCl aqueous solution 0.9% w/w (orange lines); (B) in PBS in presence of 2% (v/v) of human serum albumin (HSA) (magenta lines), and fetal bovine serum (FBS) (dark cyan lines).



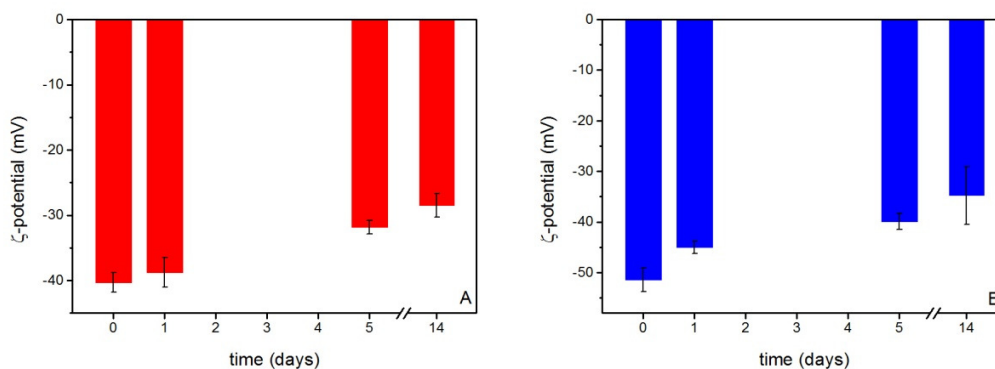


**Figure S8.** Stability of SP (A) and SAP (B) in aqueous solution. Data are reported as mean of three independent experiments  $\pm$  SD.

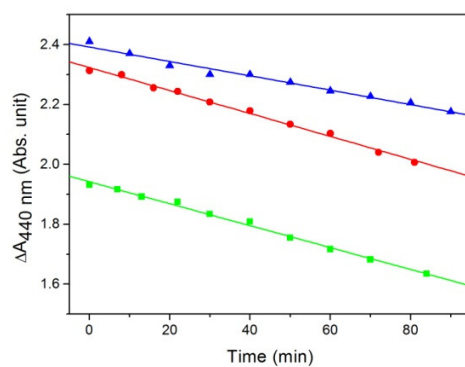


**Figure S9.** *p*-nitroso-*N,N'*-dimethylaniline (RNO) bleaching kinetics of Pheo (green squares), SP (red circles) and SAP (blue triangles) (see Experimental).

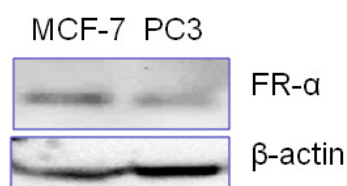


**Figure S10.** Different expression of folate receptor protein (FR-α) in MCF-7 and PC3 cells by western blotting

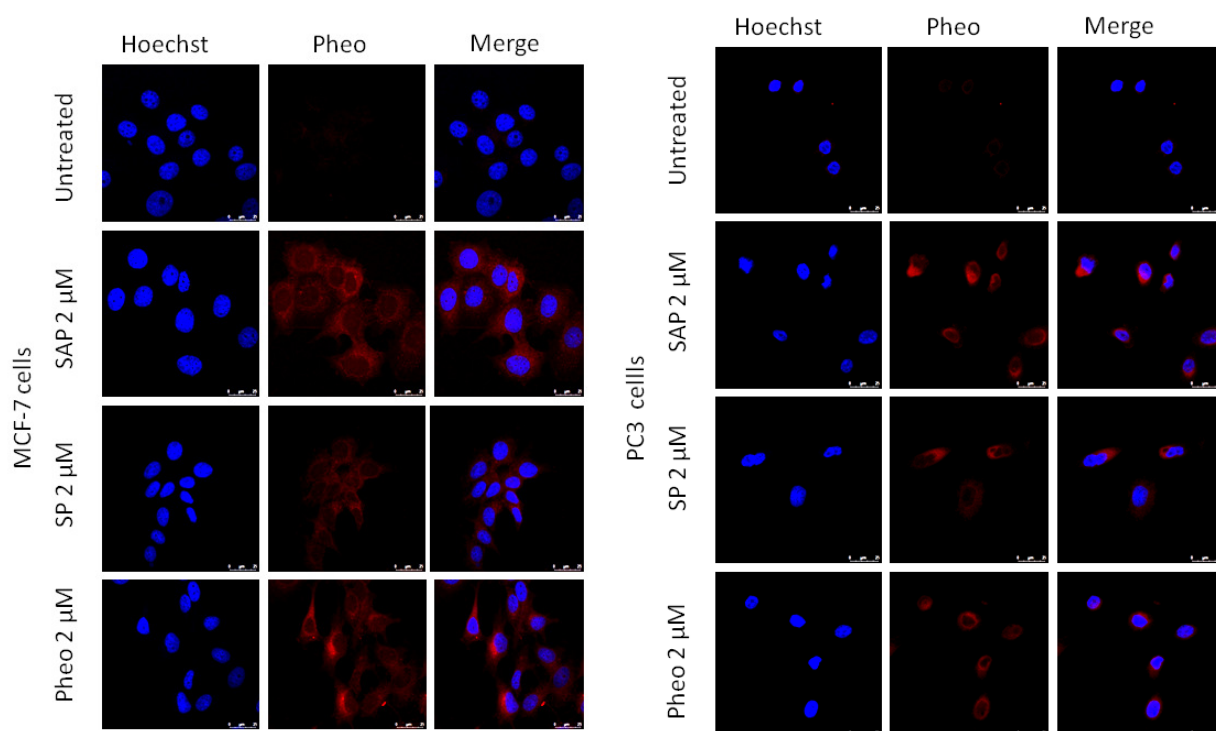


**Figure S11.** Confocal microscope images. MCF-7 (left) and PC3 cells (right) were seeded on 19 mm coverslips at a density of  $3 \times 10^5$  and  $4 \times 10^5$ , respectively. After a day, the cells were treated with SAP, SP or Pheo ( $[Pheo] = 2 \mu M$ ) for 3 h in the dark in RPMI medium without serum. For each series, the right column reports the images obtained staining nuclei with Hoechst; central column reports the images obtained by the red fluorescence emitted by Pheo and the right column represents the images obtained merging two fluorophores.

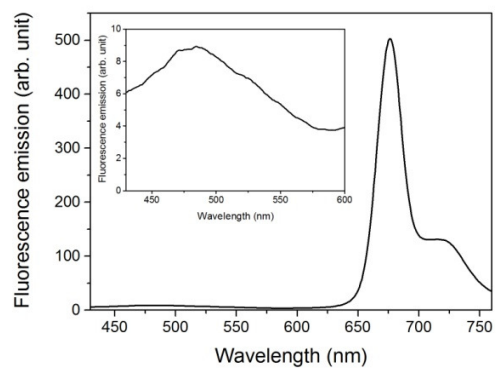


**Figure S12.** Fluorescence emission spectra of Dns-SP in aqueous solution. In the inset a magnification of emission band related to the presence of dansyl group labeling NA ( $\lambda_{\text{exc}} = 390$  nm, r.t.).

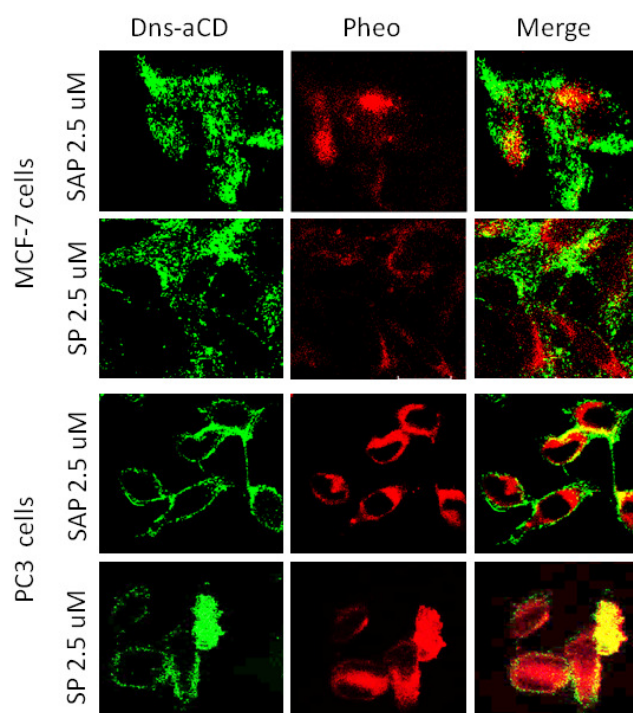


**Figure S13.** Confocal microscope images. The MCF-7 and PC3 cells were seeded on 19 mm coverslips at a density of  $3 \times 10^5$  and  $4 \times 10^5$ , respectively. After a day they were treated with Dns-SP or Dns-SAP ( $[\text{Pheo}] = 2.5 \mu\text{M}$ ) for 3h in the dark in RPMI medium w/o serum; for brevity, in the legend, Dns-amphiphilic CD is indicated as Dns-aCD, and Dns-SP and Dns-SAP as SP and SAP, respectively.

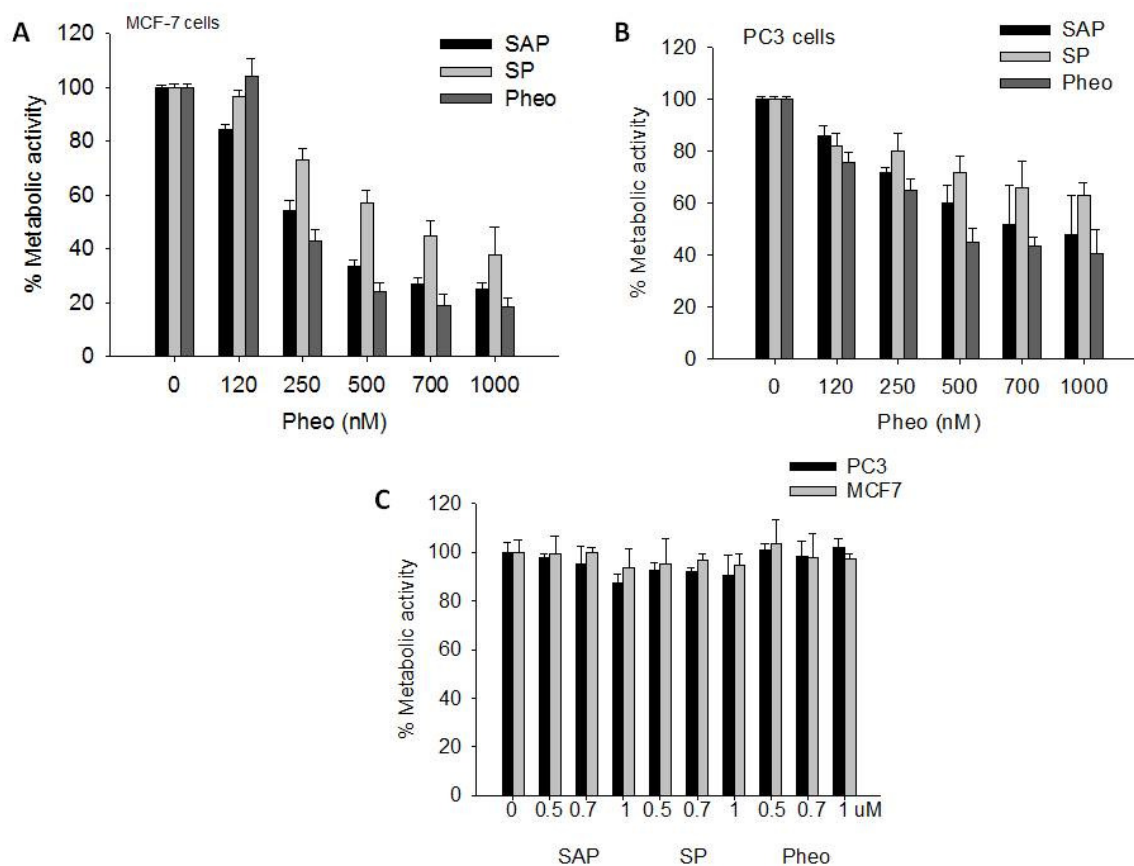


**Figure S14.** % Metabolic activity of SAP, SP and Pheo. MCF-7 (a) and PC3 (b) cells were treated for 3 h in the dark with increasing amounts of nanoassemblies (dose is expressed as concentration of entrapped Pheo) and light irradiated with a red led ( $0.9 \text{ J/cm}^2$ ). After 24 h a resazurin assay was performed; (c) % Metabolic activity of MCF-7 and PC3 cells treated with SAP, SP or Pheo for 24 h in the dark.

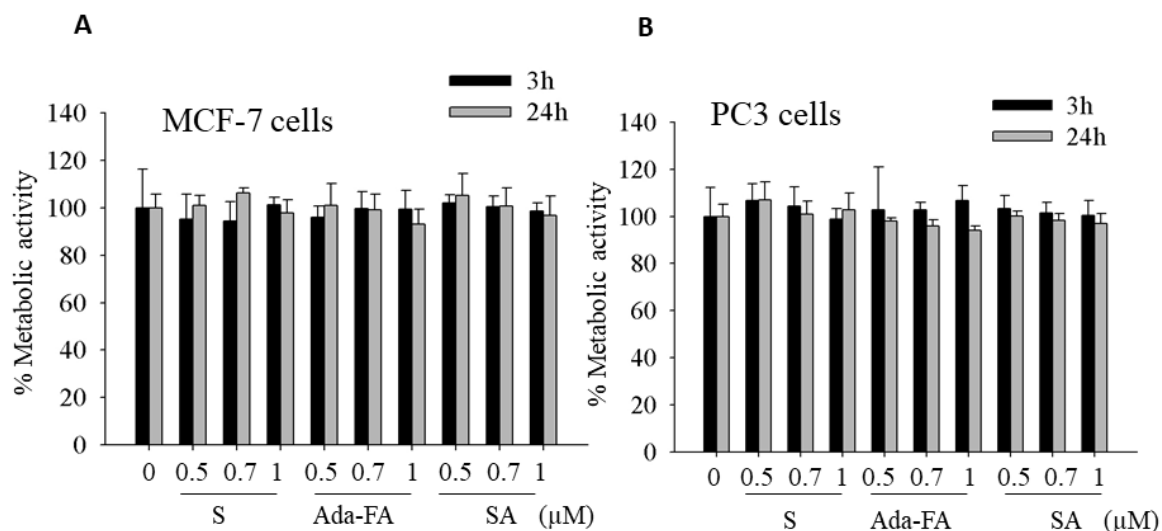


**Figure S15.** Metabolic activity (%) of S, Ada-FA and SA in MCF-7 (left) and PC3 cells (B). The cells were treated for 3 h or 24 h in the dark with increasing concentrations of the systems. S Ada-FA and SA concentrations are equivalent to those present in SAP considering EE% of entrapped Pheo and Ada-FA respectively. After 24 h a resazurin assay was performed.

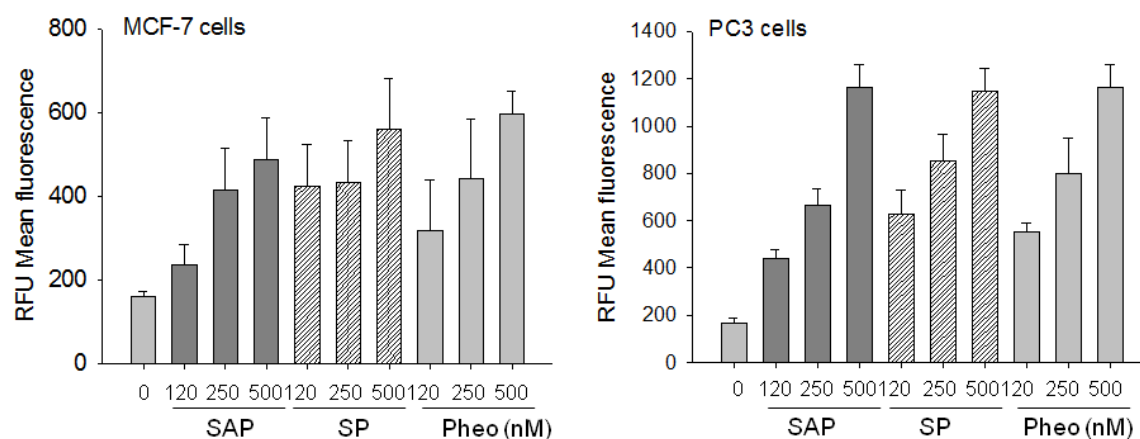


**Figure S16.** Intracellular ROS in MCF-7 and PC3 cells treated with increasing amounts of SAP, SP and Pheo.

## References

1. Beer, P. D.; Cadman, J.; Lloris, J. M.; Martínez-Máñez, R.; Soto, J.; Pardo, T.; Marcos, M. a. D., Anion interaction with ferrocene-functionalised cyclic and open-chain polyaza and aza-oxa cycloalkanes. *J. Chem. Soc., Dalton Trans.* **2000**, 0, (11), 1805-1812.
2. Samanta, A.; Tesch, M.; Keller, U.; Klingauf, J.; Studer, A.; Ravoo, B. J., Fabrication of Hydrophilic Polymer Nanocontainers by Use of Supramolecular Templates. *J. Am. Chem. Soc.* **2015**, 137, (5), 1967-1971.
3. Tarn, D.; Ferris, D. P.; Barnes, J. C.; Ambrogio, M. W.; Stoddart, J. F.; Zink, J. I., A reversible light-operated nanovalve on mesoporous silica nanoparticles. *Nanoscale* **2014**, 6, (6), 3335-3343.
4. Guaragna, A.; Chiaviello, A.; Paoletta, C.; D'Alonzo, D.; Palumbo, G.; Palumbo, G., Synthesis and Evaluation of Folate-Based Chlorambucil Delivery Systems for Tumor-Targeted Chemotherapy. *Bioconjugate Chem.* **2012**, 23, (1), 84-96.
5. Dhar, S.; Liu, Z.; Thomale, J.; Dai, H.; Lippard, S. J., Targeted Single-Wall Carbon Nanotube-Mediated Pt(IV) Prodrug Delivery Using Folate as a Homing Device. *J. Am. Chem. Soc.* **2008**, 130, (34), 11467-11476.

6. Mazzaglia, A.; Valerio, A.; Micali, N.; Villari, V.; Quaglia, F.; Castriciano, M. A.; Monsù Scolaro, L.; Giuffrè, M.; Siracusano, G.; Sciortino, M. T., Effective cell uptake of nanoassemblies of a fluorescent amphiphilic cyclodextrin and an anionic porphyrin. *Chem. Commun.* **2011**, 47, (32), 9140-9142.